

Optimization of acid orange II degradation using $\text{Fe}_{3-x}\text{Mn}_x\text{O}_4$ -MKSF catalyst in heterogeneous fenton-like reaction via response surface methodology

Amirah Annasuha Azmi¹, Rasyidah Alrozi^{1,2*}, Nor Aida Zubir^{1,2}, Mohamad Anuar Kamaruddin³

¹Chemical Engineering Studies, College of Engineering, Universiti Teknologi MARA, Cawangan Pulau Pinang, 13500, Permatang Pauh, Pulau Pinang, Malaysia

²Hybrid Nanomaterials, Interfaces & Simulation (HYMFAST), Chemical Engineering Studies, College of Engineering, Universiti Teknologi MARA, Cawangan Pulau Pinang, 13500, Permatang Pauh, Pulau Pinang, Malaysia

³Environmental Technology Division, School of Industrial Technology, Universiti Sains Malaysia, Pulau Pinang, Malaysia

ARTICLE INFO

Article history:

Received 27 January 2025

Revised 27 February 2025

Accepted 7 March 2025

Online first

Published 17 March 2025

Keywords:

Optimization

Acid orange II dye

Fenton-like reaction

$\text{Fe}_{3-x}\text{Mn}_x\text{O}_4$ -MKSF

Heterogeneous catalyst

Response surface methodology

DOI:

10.24191/esteem.v21i1March.4755.g
3039

ABSTRACT

In this study, the operational conditions for acid orange II (AOII) degradation in a heterogeneous Fenton-like reaction using a clay-supported $\text{Fe}_{3-x}\text{Mn}_x\text{O}_4$ ($\text{Fe}_{3-x}\text{Mn}_x\text{O}_4$ -MKSF) catalyst were optimized using response surface methodology (RSM). A standard RSM called a central composite design (CCD) experiment was used to determine the effects of four operational variables: pH solution, catalyst dosage, concentration of H_2O_2 and initial concentration of AOII on the percentage of AOII removal. Based on the analysis of variance (ANOVA), the model exhibited a correlation coefficient (R^2) of 0.9672 which demonstrated approximately 96% of target function variation. The optimal operational conditions were obtained at 2.5 pH solution, 0.4 g/L catalyst dosage, 15 mM H_2O_2 concentration and 35 mg/L AOII initial concentration which resulted in 86.72% of AOII degradation. The experimental results showed good agreement with the values predicted by the model at optimal conditions, exhibiting relative differences of less than 5%. These findings provide valuable insights into the interaction of four key variables affecting AOII degradation during the heterogeneous Fenton-like reaction using $\text{Fe}_{3-x}\text{Mn}_x\text{O}_4$ -MKSF catalyst.

* Corresponding author. E-mail address: rasyidah.alrozi@uitm.edu.my

1. INTRODUCTION

Acid orange II (AOII) is an azo dye containing one or more azo groups (-N=N-) bound to aromatic rings. AOII is commonly used in textile industry, which is a major contributor of water pollution in terms of spent volume, as well as colour and chemical composition of the residual wastewater [1]. The effluent from these kinds of industries usually contains a substantial amount of dye when discharged into water bodies [2,3]. Furthermore, the discharged dyes are recognized as carcinogenic and mutagenic contaminants exhibiting limited biodegradability in the environment [4]. Their dissolution in aqueous media leads to discolouration of surface waters, impeding light penetration. This, in turn, disrupts photosynthetic activity in aquatic flora, consequently impacting the food sources of marine organisms. Consequently, the release of untreated dyes poses a significant threat to both human health and aquatic ecosystems.

Recently, advanced oxidation processes (AOPs) have gained widespread attention for dye degradation [5]. AOPs generate powerful oxidising radicals, such as hydroxyl ($\bullet\text{OH}$) radicals, to degrade contaminants in wastewaters. These radicals can be produced by several AOPs, including homogeneous Fenton/Fenton-like, heterogeneous Fenton/Fenton-like, photo-Fenton, photocatalysis and ozonation [6]. Among the AOPs, the heterogeneous Fenton-like reaction is a promising alternative for the wastewater treatment. Heterogeneous Fenton-like reactions have several advantages over homogeneous processes, which are: (i) the reaction takes place at near-neutral pH; (ii) the catalysts can easily be recycled and regenerated, and (iii) it eliminates the need for the acidification and neutralisation steps, thereby avoiding sludge formation [7]. However, some heterogeneous catalysts exhibit enhanced catalytic performance in acidic environments. For instance, Lassoued et al. [8] reported that the highest degradation efficiency of AOII dye (96.5% within 12 min) was achieved at pH 3 by $\text{Fe}_{78}\text{Si}_9\text{B}_{13}$ during a Fenton-like reaction. Furthermore, Moazeni et al. [9] reported that MIL-101(Fe) acted efficiently as a catalyst for Orange G dye degradation (74% within 30 min) at pH 3 in the presence of peroxymonosulfate (PMS) as an oxidant. It was found that the acidic conditions enhanced surface protonation, thereby facilitating the generation of reactive radical species, which in turn increased the concentration of active sites and improved catalytic efficiency [10].

The performance of iron-based composite materials as catalysts in heterogeneous Fenton-like reactions is directly influenced by several parameters, including pH of the solution, concentration of oxidant, catalyst dosage, and the concentration of the organic compounds [11]. Therefore, direct interaction between these parameters using response surface methodology (RSM) is important in understanding the overall process behaviour [12]. A standard RSM which consists of a central composite design (CCD) is a statistical method that is useful for the optimization of chemical reactions and/or industrial processes and is widely used for experimental design. In fact, it will give detailed interaction between the parameters with a minimum number of required runs [13]. The CCD has been used in heterogeneous Fenton-like reactions for the optimization of methyl orange dye using Fe-MKSF [14], rhodamine B dye using magnetic nanoscale MnFe_2O_4 [12], and acid orange 7 dye using graphene oxide-iron [15] and $\text{Fe}_{3-x}\text{Co}_x\text{O}_4$ [16].

Previous research work has demonstrated that clay-supported $\text{Fe}_{3-x}\text{Mn}_x\text{O}_4$ ($\text{Fe}_{3-x}\text{Mn}_x\text{O}_4$ -MKSF) exhibits superior catalytic activity for the degradation of AOII, achieving up to 98% removal efficiency, which significantly surpasses the performance of both $\text{Fe}_{3-x}\text{Mn}_x\text{O}_4$ and Fe_3O_4 catalysts [17]. However, optimization of AOII dye degradation in a heterogeneous Fenton-like reaction by $\text{Fe}_{3-x}\text{Mn}_x\text{O}_4$ -MKSF via RSM has not been reported in the literature. Hence, the aim of the present study was to evaluate and optimise the important operational parameters (pH solution, catalyst dosage, H_2O_2 concentration and initial AOII concentration) for AOII degradation in the presence of $\text{Fe}_{3-x}\text{Mn}_x\text{O}_4$ -MKSF catalyst using CCD.

2. MATERIALS AND METHODS

2.1 Preparation of clay-supported $\text{Fe}_{3-x}\text{Mn}_x\text{O}_4$ ($\text{Fe}_{3-x}\text{Mn}_x\text{O}_4$ -MKSF) catalyst

The $\text{Fe}_{3-x}\text{Mn}_x\text{O}_4$ -MKSF catalyst was synthesised using a double boiling technique. First, 17 ml of 0.05 mol/L $\text{FeCl}_3 \cdot 6\text{H}_2\text{O}$ was preheated in a beaker at 90°C and 250 rpm. Then, 1 M of NaOH was added dropwise into the mixture until the pH reached 4. At this condition (pH 4), 0.15 g MKSF clay was added to the mixture solution to prevent the probability of the clay sticking together which may lead to the reduction of the effective surface of the clay [18]. The mixture solution was stirred for 15 minutes. The NaOH was continued to be added dropwise until the pH reached 10. The solution was aged for 1 hour. The resultant suspension was centrifuged to recover the sample and washed several times with deionized water and ethanol. Finally, the sample was dried in an oven at 90°C for 24 hours.

2.2 Experimental design

In the present study, the optimization of operational condition for AOII degradation focused on the initial concentration of H_2O_2 (5 – 45 mM), the initial concentration of dye (15 – 55 mg/L), the catalyst dosage (0.2 – 1.0 g/L) and the initial pH solution (2.0 – 4.0). These variables and their respective ranges were selected based on the preliminary studies, as summarized in Table 1. The $\text{Fe}_{3-x}\text{Mn}_x\text{O}_4$ -MKSF catalyst was added into the AOII solution at a specific range of pH. The catalytic reaction was activated by hydrogen peroxide (H_2O_2) and stirred at 300 rpm at room temperature. At the end of the experiment, the samples were filtered using 0.2 μm syringe filters. The filtrate samples were immediately analysed using UV-Vis spectrophotometer (Lamda 25, Perkin Elmer) at $\gamma_{\text{max}} = 464 \text{ nm}$. The experimental data were analysed using Design Expert software version 11 (STAT-EASE Inc. Minneapolis, USA) and CCD was used to develop a polynomial regression equation to analyse the correlation between the AOII operating variables and AOII degradation.

Table 1. Independent variable and their coded levels for CCD

Variable (factors)	Symbol	Coded variable levels				
		$-\alpha$	-1	0	+1	$+\alpha$
pH solution	<i>A</i>	2.0	2.5	3.0	3.5	4.0
Catalyst dosage (g/L)	<i>B</i>	0.2	0.4	0.6	0.8	1.0
Concentration of H_2O_2 (mM)	<i>C</i>	5.0	15.0	25.0	35.0	45.0
Concentration of AOII (mg/L)	<i>D</i>	15.0	25.0	35.0	45.0	55.0

The CCD requires three types of runs which are 2^n factorial runs, 2^n axial runs and 6 centre runs, where n represents the number of variables. For four variables; 16 factorial points, 8 axial points and 6 replicates at the centre point were employed, resulting in a total of 30 experiments, as calculated using Eq. (1) [14]. The axial points were positioned at $(\pm\alpha, 0, 0)$, $(0, \pm\alpha, 0)$ and $(0, 0, \pm\alpha)$ where α represents the axial distance from the centre.

$$N = 2^n + 2^n + n_c = 24 + 2(24) + 6 = 30 \quad (1)$$

Where N is the total number of experiments required.

3. RESULTS AND DISCUSSION

3.1 Development of regression model equation

The complete design matrices together with the response obtained from experimental work are shown in Table 2. Runs 25 to 30 at the centre point were conducted to determine the experimental error and the reproducibility of the data. Detailed relationships between the four independent variables and the corresponding response of AOII degradation were found to be well-fitted with a quadratic model. The regression of the quadratic model for AOII degradation obtained from CCD is presented in Eq. (2):

$$Y = 5.34 - 2.81A - 0.1930B + 0.056C - 0.1348D - 0.1254AD + 0.0736BC - 0.0827BD + 0.0573CD + 0.3415A^2 - 0.8963B^2 + 0.2995C^2 + 0.5053D^2 \quad (2)$$

The coefficient with one factor represents the effect of the factor, while the coefficients with two factors and those with second-order terms represent the interaction between two factors and the quadratic effect, respectively. The positive sign in front of the terms indicates a synergistic effect, whereas a negative sign indicates an antagonistic effect. Thus, from Eq. (2), it is evident that the positive sign of the concentration of H_2O_2 (C) shows a positive effect towards the response of AOII degradation. On the other hand, pH solution (A), catalyst dosage (B) and initial concentration of AOII (D) show a negative effect towards the response, which indicates that the degradation efficiency decreases when the factors increase from low level to high level.

3.2 Analysis of variance

An ANOVA analysis (Table 3) shows the significance and relationship between a response variable and one or more independent variables. The ANOVA for the regression model of AOII degradation demonstrated that the model is statistically significant owing to the low probability value as well as the calculated Fisher variation ratio value (F-value) [13,19]. If the value of Prob. >F is less than 0.05, the model terms are considered significant at 95% confidence level [14,16]. The significance of the quadratic model was verified with an F-value for AOII degradation in a heterogeneous Fenton-like reaction which corresponds to 41.83 with a p-value <0.0001. From Table 3, A , A^2 , B^2 , C^2 and D^2 factors were significant model terms whereas B , C , D , AD , BC , BD , and CD were insignificant to the response because the p-values were greater than 0.1000. The lack of fit test with p-value of 0.0673 (p-value > 0.05 implies insignificant) suggests that the model fits well with the experimental data. In addition, the ability of the quadratic polynomial model is expressed based on coefficients of determination (regression coefficients) R^2 , adjusted R^2 and predicted R^2 as well as the coefficient variation (CV) value. Interestingly, the minimum CV value for the model (9.47%), as shown in Table 4, indicates good reliability of the experimental values and acceptable variability within the data system. The model illustrated a high correlation coefficient (R^2) of 0.9672, indicating that the model can demonstrate 97% of the target function variation. The adjusted R^2 and predicted R^2 are 0.9441 and 0.8495, respectively, which reveals reasonable agreement (the difference is less than 0.2) and suggests that there are excellent correlations between the independent variables. In fact, Fig. 1. shows that the experimental data are well-fitted to the model when the predicted values obtained are quite close to the experimental values.

Table 2. Experimental design matrix for operating variable of AOII degradation

Run	Level				Operating variable				AOII degradation (%)
					Solution pH, <i>A</i>	Catalyst dosage, <i>B</i> (g/L)	Concentration of H ₂ O ₂ , <i>C</i> (mM)	Initial concentration of AOII, <i>D</i> (mg/L)	
1	-1	-1	-1	-1	2.5	0.4	15	25	92.64
2	+1	-1	-1	-1	3.5	0.4	15	25	73.30
3	-1	+1	-1	-1	2.5	0.8	15	25	90.64
4	+1	+1	-1	-1	3.5	0.8	15	25	63.00
5	-1	-1	+1	-1	2.5	0.4	35	25	97.95
6	+1	-1	+1	-1	3.5	0.4	35	25	72.40
7	-1	+1	+1	-1	2.5	0.8	35	25	90.10
8	+1	+1	+1	-1	3.5	0.8	35	25	21.80
9	-1	-1	-1	+1	2.5	0.4	15	45	96.96
10	+1	-1	-1	+1	3.5	0.4	15	45	71.00
11	-1	+1	-1	+1	2.5	0.8	15	45	85.05
12	+1	+1	-1	-1	3.5	0.8	15	45	28.12
13	-1	-1	+1	+1	2.5	0.4	35	45	98.29
14	+1	-1	+1	+1	3.5	0.4	35	45	62.30
15	-1	+1	+1	+1	2.5	0.8	35	45	91.35
16	+1	+1	+1	+1	3.5	0.8	35	45	20.50
17	- α	0	0	0	2	0.6	25	35	95.82
18	+ α	0	0	0	4	0.6	25	35	20.00
19	0	- α	0	0	3	0.2	25	35	55.89
20	0	+ α	0	0	3	1	25	35	40.12
21	0	0	- α	0	3	0.6	5	35	22.03
22	0	0	+ α	0	3	0.6	45	35	25.20
23	0	0	0	- α	3	0.6	25	15	28.42
24	0	0	0	+ α	3	0.6	25	55	29.97
25	0	0	0	0	3	0.6	25	35	56.00
26	0	0	0	0	3	0.6	25	35	21.57
27	0	0	0	0	3	0.6	25	35	23.66
28	0	0	0	0	3	0.6	25	35	27.89
29	0	0	0	0	3	0.6	25	35	27.84
30	0	0	0	0	3	0.6	25	35	28.55

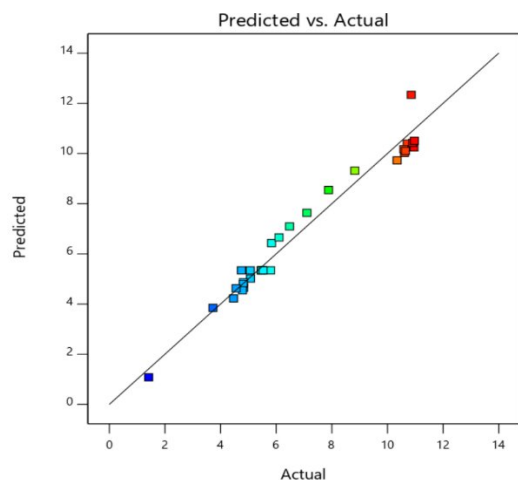


Fig. 1. Predicted versus actual percentage of AOII degradation

Table 3. Analysis of variance (ANOVA) for the regression model of AOII degradation

Source	Sum of Square	DF	Mean Square	F-Value	Prob>F	
Model	219.0900	12	18.2600	41.8300	<0.0001	Significant
<i>A</i>	190.0500	1	190.0500	435.4000	<0.0001	
<i>B</i>	0.8936	1	0.8936	2.0500	0.1706	
<i>C</i>	0.0770	1	0.0770	0.1765	0.6797	
<i>D</i>	0.4363	1	0.4363	0.9995	0.3315	
<i>AD</i>	0.2516	1	0.2516	0.5764	0.4581	
<i>BC</i>	0.0867	1	0.0867	0.1987	0.6614	
<i>BD</i>	0.1094	1	0.1094	0.2507	0.6230	
<i>CD</i>	0.0526	1	0.0526	0.1205	0.7328	
<i>A</i> ²	3.2000	1	3.2000	7.3300	0.0150	
<i>B</i> ²	22.0300	1	22.0300	50.4800	<0.0001	
<i>C</i> ²	2.4600	1	2.4600	5.6400	0.0296	
<i>D</i> ²	7.0000	1	7.0000	16.0400	0.0009	
Residual	7.4200	17	0.4365			
Lack of Fit	6.7200	12	0.5604	4.0300	0.0673	Not Significant
Pure Error	0.6959	5	0.1392			
Correlation Total	226.5100	29				

Table 4. Fit statistic

Standard Deviation	Mean	Coefficient of Variation (<i>CV</i>)	Regression, <i>R</i> ²	Adjusted <i>R</i> ²	Predicted <i>R</i> ²	Adeq Precision
0.6607	6.98	9.47	0.9672	0.9441	0.8495	25.8814

3.3 Interaction effects between parameters

The two-dimensional contour plot displayed the relationships between pH solution and initial concentration of AOII (Fig. 2. (a)), catalyst dosage and H₂O₂ concentration (Fig. 2. (b)), catalyst dosage and initial concentration of AOII (Fig. 2. (c)) and H₂O₂ concentration and initial concentration of AOII (Fig. 2. (d)) towards AOII degradation. From Fig. 2. (a), the degradation efficiency of AOII was increased up to 80% after 180 minutes at pH in the range of 2.5 to 3.0 and the initial concentration of AOII was in between 25 to 35 mg/L. The lower the pH, the better the degradation efficiency with lower AOII concentration. It indicated that the degradation of AOII was significantly influenced in an acidic medium (pH 2.5 to 3.0). The results obtained were in agreement with previous studies which claimed that H₂O₂ and ferrous ions are more stable when pH is lower than 3.0 [20,21]. According to Blanco et al. [21], in alkaline medium, H₂O₂ may decompose to oxygen and water and lose its oxidation ability. Meanwhile, when the catalyst dosage is in the range of 0.6 to 0.7 g/L and the H₂O₂ concentration is in between 20 to 25 mM, the AOII degradation achieved up to 60% (Fig. 2. (b)). This finding indicates that both catalyst dosage and H₂O₂ concentration may influence the reactivity of the catalyst towards AOII degradation. Adding more catalyst enhances the availability of active sites for H₂O₂ activation, thereby promoting the generation of reactive radical species (•OH radicals) and consequently improving the degradation rate of AOII [15]. However, excessive catalyst dosage can accelerate the H₂O₂ activation, and the generation of abundant reactive radicals would react with each other [22] and, hence inhibit the degradation of AOII.

From Fig. 2. (c), catalyst dosage is within the range of 0.6 to 0.7 g/L and the initial concentration of AOII is 30 to 40 mg/L leading to 60% degradation efficiency of AOII. Low concentrations of AOII are favourable to AOII degradation. On the contrary, the high initial concentration of AOII resulted in the saturation of active sites on the catalyst. This phenomenon restricts the interaction between the available active sites and H₂O₂, which consequently hinders the efficient generation of •OH radicals [23]. On the other hand, high degradation of AOII was achieved (up to 75%) at H₂O₂ concentrations ranging between 20 to 25 mM and concentrations of AOII at 25 to 35 mg/L (Fig. 2. (d)). Optimum H₂O₂ concentration during catalysis is crucial since excessive H₂O₂ may cause an unfavourable reaction between H₂O₂ and •OH radicals, generating hydroperoxyl radicals (•OOH), which are less reactive than •OH radicals [24,25]. The •OOH radicals are then reacting with •OH radicals to produce oxygen and water. The quenching effect of •OH radicals by H₂O₂ inhibit the Fenton-like reaction [24]

Based on the above discussion, the contour plot enables to provide an in-depth understanding on the impact of the relationship between pH solution, catalyst dosage, H₂O₂ concentration, and initial AOII concentration on AOII degradation efficiency during the heterogeneous Fenton-like reaction in the presence of Fe_{3-x}Mn_xO₄-MKSF catalyst. These findings, reinforced by regression analysis and ANOVA, emphasised the importance of an integrated approach to optimizing AOII degradation efficiency.

3.4 Optimization and model validation

In this study, the optimum operational conditions for the regression model were found to be at a 2.5 pH solution, 0.4 g/L catalyst dosage, 15 mM H₂O₂ concentration and 35 mg/L AOII initial concentration which subsequently resulted in 86.72% of AOII degradation. Table 5 presents the validation experiments for AOII degradation under these optimal conditions. Five validation runs were conducted which provide the expected values of the actual percentage of AOII degradation, under the experimental conditions, with a negligible percentage of errors. For example, in Run 1, the actual AOII degradation efficiency was 86.98%, slightly higher than the predicted efficiency of 86.72%, yielding a minor error of 0.30%. The significant correlation between experimental and predicted values validates the reliability of the quadratic model for accurately predicting the AOII degradation under optimum operational conditions.

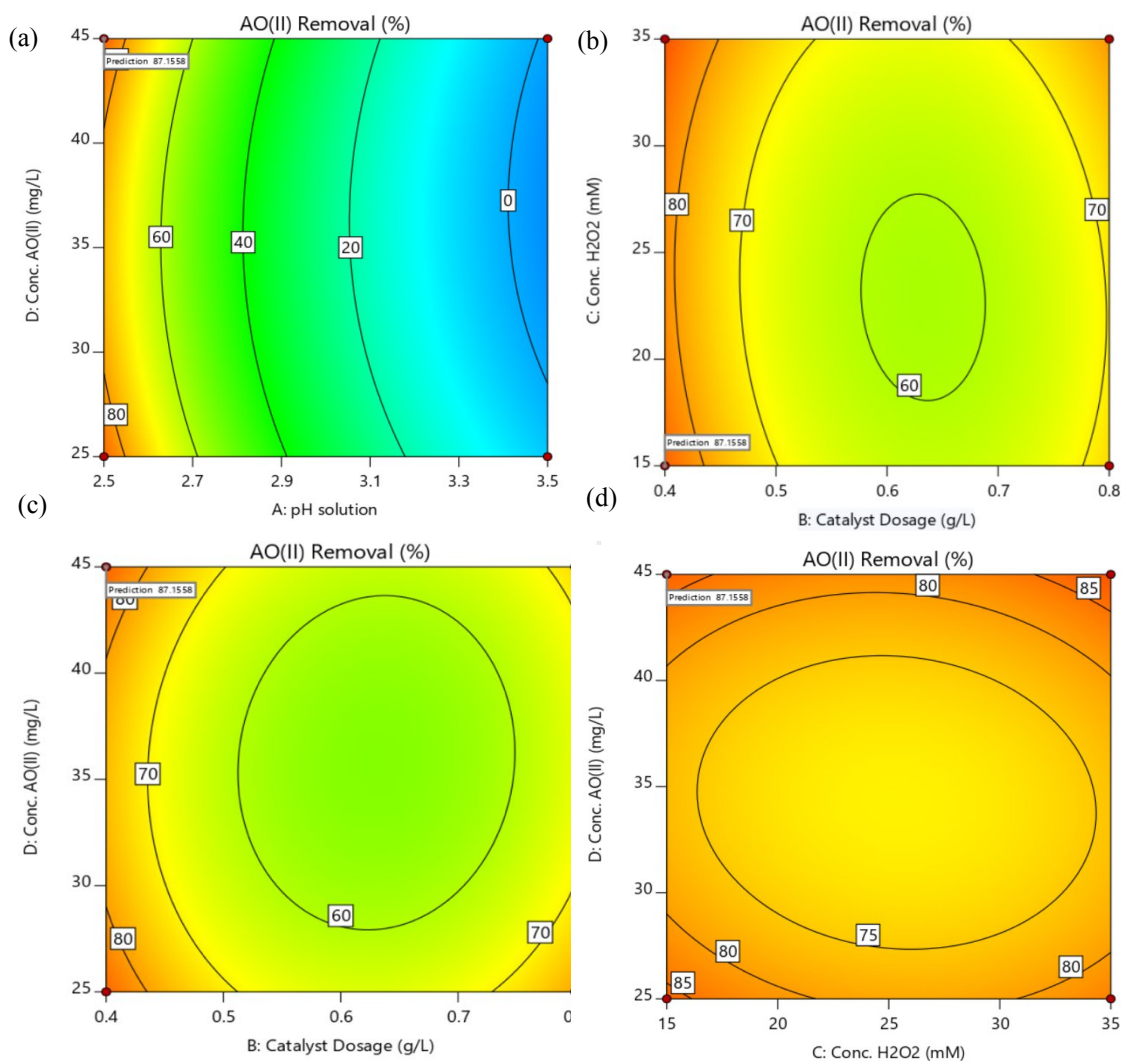


Fig. 2. Two-dimensional response (contour) for the interaction between (a) pH solution and initial concentration of AOII (AD); (b) catalyst dosage and H_2O_2 concentration (BC); (c) catalyst dosage and initial concentration of AOII (BD), and (d) H_2O_2 concentration and initial concentration of AOII (CD) towards AOII degradation

The consistently low percentage errors ($<5\%$) across all validation trials demonstrate the dependability and efficacy of the model-derived optimal operational conditions for AOII degradation. The reproducibility of these optimum conditions is evident from consistent experimental results, highlighting the suitability of the regression model for practical wastewater treatment applications. These findings confirm the model's predictive capacity for oxidative degradation of AOII using $Fe_{3-x}Mn_xO_4$ -MKSF catalyst in a heterogeneous Fenton-like reaction.

Table 5. Validation run of the optimum operating condition for AOII degradation in presence of $\text{Fe}_{3-x}\text{Mn}_x\text{O}_4$ -MKSF catalyst

Run	pH solution, <i>A</i>	Catalyst dosage, <i>B</i> (g/L)	H_2O_2 concentration, <i>C</i> (mM)	Initial of AOII concentration, <i>D</i> (mg/L)	AOII degradation (%)		Error (%)
					Predicted	Experimental	
1	2.5	0.4	15	35	86.72	86.98	0.30
2	2.5	0.4	15	35	86.72	87.12	0.46
3	2.5	0.4	15	35	86.72	87.75	1.17
4	2.5	0.4	15	35	86.72	87.98	1.43
5	2.5	0.4	15	35	86.72	88.36	1.86

For comparison purposes, Table 6 displays the catalytic performance of $\text{Fe}_{3-x}\text{Mn}_x\text{O}_4$ -MKSF against various Fe-based catalysts in heterogeneous Fenton-like reactions. The catalytic performance of $\text{Fe}_{3-x}\text{Mn}_x\text{O}_4$ -MKSF in this work for AOII degradation is comparable to other Fe-based catalysts reported in the literature. Thus, $\text{Fe}_{3-x}\text{Mn}_x\text{O}_4$ -MKSF catalyst shows strong potential to be utilised as a heterogeneous catalyst for water/wastewater remediation.

Table 6. Catalytic performance of various Fe-based catalysts for AOII degradation

Catalyst	Parameter conditions				Degradation efficiency (%)	Ref.
	pH solution	Catalyst dosage (g/L)	Oxidant concentration (mM)	Initial of AOII dye concentration (mg/L)		
$\text{Fe}_{29}\text{Co}_{28}\text{Ni}_{28}\text{B}_{14}\text{Si}_1$	3	0.5	$[\text{H}_2\text{O}_2] = 5.0$ mM	25	100 in 4 min	[26]
MIL-101(Fe)	3	0.015	$[\text{PMS}] = 0.05$ mM	11	74% in 30 min	[9]
$\text{Fe}_{78}\text{Si}_9\text{B}_{13}$	3	4.0	$[\text{H}_2\text{O}_2] = 1.0$ mM	20	96.5% in 12 min	[8]
$\text{Fe}_{78}\text{Si}_8\text{B}_{14}$	6.7	1.0	$[\text{PS}] = 10$ mM	200	99% in 8 min	[27]
MIL-100(Fe)/GO	3	0.5	$[\text{H}_2\text{O}_2] = 8$ mM	50	99% in 2 hr	[11]
CaCuFeO_3	6.4	1.0	$[\text{H}_2\text{O}_2] = 22$ mM	35	97% in 1 hr	[28]
$\text{Fe}_{3-x}\text{Mn}_x\text{O}_4$ -MKSF	2.5	0.4	$[\text{H}_2\text{O}_2] = 15$ mM	35	86.7% in 3 hr	This work

4. CONCLUSION

Response surface methodology was successfully used to investigate the effects of pH solution, catalyst dosage, H_2O_2 concentration, and initial concentration of AOII on the percentage degradation of AOII using $\text{Fe}_{3-x}\text{Mn}_x\text{O}_4$ -MKSF catalyst in a heterogeneous Fenton-like reaction. The optimum operational condition of AOII degradation was obtained at pH solution of 2.5, a catalyst dosage of 0.4 g/L, H_2O_2 concentration of 15 mM and an AOII initial concentration of 35 mg/L, which subsequently resulted in 86.72% of AOII degradation. The interaction between these parameters was found to be significantly correlated with the response. In fact, the experimental values were in good agreement with the predicted values with less than

5% differences. These findings indicate good interaction between four operational variables (pH solution catalyst dosage, H₂O₂ concentration and AOII initial concentration) towards AOII degradation during the process of optimization of the heterogeneous Fenton-like reaction using Fe_{3-x}Mn_xO₄-MKSF catalyst. The optimised operational parameters and validated models in this study may enhance the potential for industrial wastewater treatment applications.

5. ACKNOWLEDGEMENTS

The authors would like to acknowledge the Ministry of Higher Education Malaysia (MOHE) and Universiti Teknologi MARA Cawangan Pulau Pinang for the financial support under the Fundamental Research Grant Scheme (FRGS/1/2018/TK05/UITM/02/12).

6. CONFLICT OF INTEREST

The authors affirm that there is no conflict of interest pertaining to the publication of this paper.

7. AUTHORS' CONTRIBUTIONS

Rasyidah Alrozi: Conceptualisation, methodology, formal analysis, investigation and writing the original draft; **Amirah Annasuha Azmi:** Material preparation, data collection and analysis; **Nor Aida Zubir:** Conceptualisation, methodology, resource, analysis, validation, writing-review and editing; **Mohamad Anuar Kamaruddin:** Validation, writing-review and editing.

8. REFERENCES

- [1] J. Zhou and H. Meifang, "Degradation of Orange II by the Fe⁰/H₂O₂ system," *IOP Conf. Ser. Earth Environ. Sci.*, vol. 526, pp. 1–9, 2020, doi: 10.1088/1755-1315/526/1/012062.
- [2] M. A. Kamaruddin, M. S. Yusoff, H. A. Aziz, and R. Alrozi, "Preparation and characterization of activated carbon embedded clinoptilolite adsorbent for colour removal from textile effluent," *J. Mater. Chem. Eng.*, vol. 2, pp. 1–10, 2014, doi: 10.12983/ijrsin-2013-p037-047
- [3] R. Alrozi, N. A. Zamanhuri, and M. S. Osman, "Adsorption of reactive dye Remazol Brilliant Blue R from aqueous solutions by rambutan peel," 2012, doi: 10.1109/SHUSER.2012.6268855.
- [4] D. Goswami, J. Mukherjee, C. Mondal, and B. Bhunia, "Bioremediation of azo dye : A review on strategies, toxicity assessment, mechanisms, bottlenecks and prospects," *Sci. Total Environ.*, vol. 954, p. 176426, 2024, doi: 10.1016/j.scitotenv.2024.176426.
- [5] A. Iqbal, A. Yusaf, M. Usman, T. Hussain Bokhari, and A. Mansha, "Insight into the degradation of different classes of dyes by advanced oxidation processes; a detailed review," *Int. J. Environ. Anal. Chem.*, vol. 104, no. 17, pp. 5503–5537, 2024, doi: 10.1080/03067319.2022.2125312
- [6] D. B. Miklos, C. Remy, M. Jekel, K. G. Linden, J. E. Drewes, and U. Hübner, "Evaluation of advanced oxidation processes for water and wastewater treatment—A critical review," *Water Res.*, vol. 139, pp. 118–131, 2018, doi: 10.1016/j.watres.2018.03.042
- [7] Y. Zhu, R. Zhu, Y. Xi, J. Zhu, G. Zhu, and H. He, "Strategies for enhancing the heterogeneous Fenton catalytic reactivity: A review," *Appl. Catal. B Environ.*, vol. 255, p. 117739, 2019, doi: 10.1016/j.apcatb.2019.05.041
- [8] A. Lassoued, L. J. Liu, and J. F. Li, "Removal of acid orange II azo dyes using Fe-based metallic glass catalysts by Fenton-like process," *J. Mater. Sci.*, vol. 57, no. 3, pp. 2039–2052, 2022, doi: 10.1007/s10853-021-06669-5.
- [9] M. Moazeni, S. M. Hashemian, M. Sillanpää, A. Ebrahimi, and K. H. Kim, "A heterogeneous

- peroxymonosulfate catalyst built by Fe-based metal-organic framework for the dye degradation,” *J. Environ. Manage.*, vol. 303, p. 113897, 2022, doi: 10.1016/j.jenvman.2021.113897.
- [10] Z. Liu, Y. Zhang, J. Lee, and L. Xing, “A review of application mechanism and research progress of Fe/montmorillonite-based catalysts in heterogeneous Fenton reactions,” *J. Environ. Chem. Eng.*, vol. 12, no. 2, p. 112152, 2024, doi: 10.1016/j.jece.2024.112152.
- [11] J. Tang and J. Wang, “Fe-based metal organic framework/graphene oxide composite as an efficient catalyst for Fenton-like degradation of methyl orange,” *RSC Adv.*, vol. 7, no. 80, pp. 50829–50837, 2017, doi: 10.1039/c7ra10145g.
- [12] H. Yan et al., “Magnetic nanoscale MnFe_2O_4 as heterogeneous Fenton-like catalyst for rhodamine B degradation: efficiency, kinetics and process optimization,” *J. Iran. Chem. Soc.*, vol. 20, no. 8, pp. 2043–2055, 2023, doi: 10.1007/s13738-023-02823-9.
- [13] M. A. Ahmad and R. Alrozi, “Optimization of rambutan peel based activated carbon preparation conditions for Remazol Brilliant Blue R removal,” *Chem. Eng. J.*, vol. 168, no. 1, 2011, doi: 10.1016/j.cej.2011.01.005.
- [14] N. Hidayati Abdullah, N. Aida Zubir, R. Alrozi, N. Nasuha, and H. Hassan, “Optimization of oxidative MO’s degradation in heterogeneous Fenton-like reaction using Fe-MKSF,” *Mater. Today Proc.*, vol. 5, no. 10, pp. 21956–21963, 2018, doi: 10.1016/j.matpr.2018.07.056.
- [15] N. A. Zubir, C. Yacou, X. Zhang, and J. C. Diniz da Costa, “Optimisation of graphene oxide – iron oxide nanocomposite in heterogeneous Fenton-like oxidation of Acid Orange 7,” *J. Environ. Chem. Eng.*, vol. 2, no. 3, pp. 1881–1888, 2014, doi: 10.1016/j.jece.2014.08.001.
- [16] M. Z. Ibrahim, R. Alrozi, N. A. Zubir, N. A. Bashah, S. A. M. Ali, and N. Ibrahim, “Optimization of Acid Orange 7 Degradation in Heterogeneous Fenton-like Reaction Using $\text{Fe}_{3-x}\text{Co}_x\text{O}_4$ Catalyst,” *IOP Conf. Ser. Mater. Sci. Eng.*, vol. 358, pp. 1–6, 2018, doi: 10.1088/1757-899X/358/1/012020.
- [17] R. Alrozi, N. A. Zubir, N. Amir, N. N. A. Abdul Rahman, and M. A. Kamaruddin, “Heterogeneous fenton-like reaction using $\text{Fe}_{3-x}\text{Mn}_x\text{O}_4$ -MKSF composite catalyst for degradation of acid orange II dye,” in *Journal of Physics: Conference Series*, 2019, vol. 1349, no. 1, doi: 10.1088/1742-6596/1349/1/012142.
- [18] N. A. Zubir, C. Yacou, J. Motuzas, X. Zhang, and J. C. Diniz Da Costa, “Structural and functional investigation of graphene oxide- Fe_3O_4 nanocomposites for the heterogeneous Fenton-like reaction,” *Sci. Rep.*, vol. 4, pp. 1–8, 2014, doi: 10.1038/srep04594.
- [19] J. Mejjide, E. Rosales, M. Pazos, and M. A. Sanromán, “p-Nitrophenol degradation by electro-Fenton process: pathway, kinetic model and optimization using central composite design,” *Chemosphere*, vol. 185, pp. 726–736, 2017, doi: 10.1016/j.chemosphere.2017.07.067
- [20] S. Kalal, A. Pandey, R. Ameta, and P. B. Punjabi, “Heterogeneous photo-Fenton-like catalysts $\text{Cu}_2\text{V}_2\text{O}_7$ and $\text{Cr}_2\text{V}_4\text{O}_{13}$ for an efficient removal of azo dye in water,” *Cogent Chem.*, vol. 2, no. 1, pp. 1–12, 2016, doi: 10.1080/23312009.2016.1143344.
- [21] M. Blanco, A. Martinez, A. Marcaide, E. Aranzabe, and A. Aranzabe, “Heterogeneous Fenton catalyst for the efficient removal of azo dyes in water,” *Am. J. Anal. Chem.*, vol. 5, p. 490, 2014, doi: 10.4236/ajac.2014.58058
- [22] H. Chen, Y. Xu, K. Zhu, and H. Zhang, “Understanding oxygen-deficient $\text{La}_2\text{CuO}_{4-\delta}$ perovskite activated peroxymonosulfate for bisphenol A degradation: The role of localized electron within oxygen vacancy,” *Appl. Catal. B Environ.*, vol. 284, no. November 2020, p. 119732, 2021, doi: 10.1016/j.apcatb.2020.119732.
- [23] Y. Rao, F. Han, Q. Chen, D. Wang, D. Xue, and H. Wang, “Efficient degradation of diclofenac by LaFeO_3 -Catalyzed peroxymonosulfate oxidation-kinetics and toxicity assessment,” *Chemosphere*, vol. 218, pp. 299–307, 2019, doi: 10.1016/j.chemosphere.2018.11.105.
- [24] M. Fayazi, M. Ali, D. Afzali, and A. Mostafavi, “Enhanced Fenton-like degradation of methylene blue by magnetically activated carbon / hydrogen peroxide with hydroxylamine as Fenton enhancer,” *J. Mol. Liq.*, vol. 216, pp. 781–787, 2016, doi: 10.1016/j.molliq.2016.01.093.
- [25] J. H. Ramirez et al., “Fenton-like oxidation of Orange II solutions using heterogeneous catalysts

- based on saponite clay,” *Appl. Catal. B Environ.*, vol. 71, no. 1–2, pp. 44–56, 2007, doi: 10.1016/j.apcatb.2006.08.012.
- [26] S. Tiwari, W. H. Ryu, K. J. Kim, and E. S. Park, “Development of (Fe-Co-Ni)-Si-B metallic glass catalyst for promoting degradation of acid orange II azo-dye,” *J. Alloys Compd.*, vol. 961, p. 171027, 2023, doi: 10.1016/j.jallcom.2023.171027.
- [27] L. Ji, R. Yu, W. Qiu, and J. Liu, “Excellent Catalytic Performance of FeSiBPY Amorphous Alloy Ribbons in the Degradation of Different Structure Dyes,” *Catal. Letters*, vol. 155, no. 3, pp. 1–18, 2025, doi: 10.1007/s10562-025-04954-5.
- [28] R. Alrozi et al., “Functional role of B-site substitution on the reactivity of CaMFeO_3 (M = Cu, Mo, Co) perovskite catalysts in heterogeneous Fenton-like degradation of organic pollutant,” *J. Taiwan Inst. Chem. Eng.*, vol. 143, p. 104675, 2023, doi: 10.1016/j.jtice.2023.104675.



© 2025 by the authors. Submitted for possible open access publication under the terms and conditions of the Creative Commons Attribution (CC BY) license (<http://creativecommons.org/licenses/by/4.0/>).